Three-dimensional visualization of thoracodorsal artery perforators using photoacoustic imaging

AUTHOR(S):

Shimizu, Hanako; Saito, Susumu; Yoshikawa, Aya; Sekiguchi, Hiroyuki; Tsuge, Itaru; Morimoto, Naoki; Toi, Masakazu

CITATION:

Shimizu, Hanako ...[et al]. Three-dimensional visualization of thoracodorsal artery perforators using photoacoustic imaging. Journal of Plastic, Reconstructive & Aesthetic Surgery 2022, 75(9): 3166-3173

ISSUE DATE:

2022-09-01

URL:

http://hdl.handle.net/2433/277544

Journal of Plastic, Reconstructive & Aesthetic Surgery 75 (2022) 3166–3173

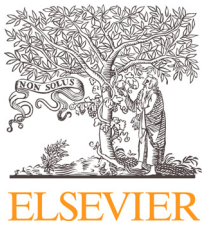

Three-dimensional visualization of thoracodorsal artery perforators using photoacoustic imaging☆,☆☆

Hanako Shimizu[a], **Susumu Saito**[b,*], **Aya Yoshikawa**[a], **Hiroyuki Sekiguchi**[c], **Itaru Tsuge**[b], **Naoki Morimoto**[b], **Masakazu Toi**[a]

[a] *Department of Breast Surgery, Graduate School of Medicine, Kyoto University, Kyoto, Japan*
[b] *Department of Plastic and Reconstructive Surgery, Graduate School of Medicine and Faculty of Medicine, Kyoto University*
[c] *Department of Diagnostic Imaging and Nuclear Medicine, Graduate School of Medicine, Kyoto University, Kyoto, Japan*

Received 29 April 2022; accepted 7 June 2022

KEYWORDS
Flap;
Perforators;
Photoacoustic imaging;
Thoracodorsal artery;
Three dimensions

Summary *Introduction:* Diagnostic imaging modalities to evaluate the three-dimensional distribution of thoracodorsal artery perforators (TDAPs) are lacking. In this study, TDAPs were visualized and characterized using photoacoustic imaging.
Material and methods: In this study, 34 sites in the lateral chest wall of 18 individuals were analyzed. The region extending 5 cm ventral and 5 cm dorsal to the lateral edge of the latissimus dorsi (LD) and 5–15 cm from the posterior axillary fold was scanned using photoacoustic imaging. The largest perforator closest to the edge of the LD was characterized. The location of the stem portion and the orientation of the longest cutaneous branch of the perforator were described. The relationship between the maximal depth of delineation on photoacoustic images and the depth of the deep fascia was assessed.
Results: On average, 2.6 perforators (range, 1–5 perforators) were visualized in the region of interest. The distribution of the TDAP stem portion was similar to that in previous studies. Cutaneous branches were preferentially oriented in a medial-caudal direction. The length of

☆Name and address of the department or institution to which the work should be attributed, Graduate School of Medicine, Kyoto University, Kyoto, Japan.
☆☆details of any meeting at which the work was presented, wholly or in part This study has not been presented at any meeting.

* Corresponing author at: Department of Plastic and Reconstructive Surgery, Kyoto University, 54, Kawahara-cho, Shogoin, Sakyo-ku, Kyoto, Japan, 606-8501.
E-mail address: susumus@kuhp.kyoto-u.ac.jp (S. Saito).

https://doi.org/10.1016/j.bjps.2022.06.016

delineated cutaneous branches varied (range, 7–78 mm) depending on the thickness of the subcutaneous layer. Vessels under the LD were observed when the subcutaneous layer was thin. *Conclusion:* Photoacoustic imaging can successfully visualize TDAPs in three dimensions. Visualization of TDAPs varied by the thickness of the subcutaneous layer. A thin deep fascia of the LD might be a cause of deep laser penetration.

Introduction

Angrigiani et al. first described the thoracodorsal artery perforator (TDAP) flap in 1995.[1] It is a skin flap supplied by perforators from the thoracodorsal artery. The TDAP flap is used as a pedicled flap in breast reconstruction.[2] It is also indicated as a free flap for the reconstruction of anatomically thin, flat tissues, such as tissues in the head and neck, axilla, and extremities.[3-5] Low donor site morbidity is an advantage of the TDAP flap, characterized by the preservation of both the latissimus dorsi (LD) muscle and thoracodorsal nerve; a low incidence of seroma is another advantage.[6] TDAPs originate from the descending branch of the thoracodorsal artery, which travels along the lateral edge of the LD. The most proximal perforator is called the first perforator.[1] The first perforator is reportedly routinely observed and reliable, owing to its thick diameter of 0.5 mm. After passing the fascia, the first perforator immediately branches and runs in the subcutaneous layer in a medial-caudal direction. Thus, its vascular territory is limited primarily to an area extending medially and caudally in the shape of a fan, called the primary zone.[7] The area surrounding the primary zone, called the secondary zone, is supplied by vascular networks from the adjacent perforators. Accordingly, preoperative identification of the course of the first perforator of the thoracodorsal artery and its connection with the surrounding vascular network is imperative for safely raising a TDAP flap. However, a lack of diagnostic imaging modalities to evaluate the three-dimensional distribution of TDAPs within the subcutaneous layer *in vivo* prevents the widespread use of TDAP flap procedures.

Photoacoustic imaging is an emerging method that uses near-infrared pulse laser beams and ultrasound to visualize blood vessels.[8] Using this technique, cutaneous microvessels can be visualized in three dimensions without the use of contrast medium. To date, photoacoustic imaging has been used for anterolateral thigh perforators,[9] digital arteries,[10] and mammary gland tumor angiogenesis.[11,12] Although the application of photoacoustic imaging to the vasculature in the living body has been reported, visualization characteristics depend on the body site.[13] In this study, TDAPs were visualized and characterized using photoacoustic imaging.

Subjects and methods

This prospective study was conducted with the approval of the ethics review board of the Kyoto University Graduate School of Medicine, Kyoto, Japan (approval number: C1366). All participants provided written informed consent. This study was implemented in accordance with the Declaration of Helsinki.

This study included healthy volunteers and patients with benign breast diseases aged ≥20 years at the time of providing consent. Pregnant or breastfeeding women, individuals who take photosensitizing agents, and individuals with a history of chemotherapy, a cardiac pacemaker, a health condition of the American Society of Anesthesiologists Physical Status Classification System class ≥4, difficulty in maintaining the position during the examination, or infection at the scan site were all excluded. The planned sample size was 25 individuals, which was based on the sample size and anatomical variability found in previous studies[14-16] on TDAPs and a 20% attrition rate.

In this study, the posterior axillary fold and the lateral edge of the LD were used as landmarks for anatomical identification. Lines parallel to the posterior axillary fold were marked on the body at 5 cm intervals. After identification of the lateral edge of the LD using ultrasound, the area extending 5–15 cm caudally from the posterior axillary fold and 5 cm ventrally and 5 cm dorsally from the lateral edge of the LD was defined as the region of interest for analysis. This setting was based on the location of the first thoracodorsal perforator reported in the literature: 6–15 cm caudally from the posterior axillary fold and 2–3 cm from the lateral edge of the LD.[1,15,16] These landmarks were noted on the skin using purple ink, which was detectable on photoacoustic images.

Prior to photoacoustic imaging, ultrasound examination was performed. Study participants were placed in the lateral position, with the upper limb elevated to 90° The lateral edge of the LD was identified and marked with the same ink used for landmark marking. To assess the impact of the thickness of the subcutaneous layer and the muscle belly of the LD on the visibility of vessels in photoacoustic images, the depth from the skin surface to the deep fascia and the deepest portion of the muscle were measured 2 cm dorsal to the lateral edge of the LD and 10 cm caudal to the posterior axillary fold. Using the color Doppler mode, the region of interest was searched for perforators. The sites at which the identified perforators emerged through the level of the deep fascia (stem portion) were marked for comparison with those on photoacoustic images. The course of each identified perforator was tracked from the stem portion to the most distal portion.

The PAI-05 photoacoustic imaging system (Canon, Japan)[13] was equipped with a cup-shaped scanner with light emission from a near-infrared laser (Q-switched Nd:YAG laser with a wavelength of 797 nm) at the center and multiple ultrasonic transducers in the periphery. The scanner was filled with de-aired water for the smooth transmission of ul-

trasonic waves. The maximum laser power was restricted to <65% of the maximum permissible exposure limit (15 mJ/cm^2 at a 20 Hz repetition rate) recommended by the American National Standards Institute[17]. The required scanning time was approximately 5 min for an 18 cm × 18 cm area. The system can delineate vessels ≥0.5 mm in diameter. The examination was performed with the study participant in the lateral position, with the lateral chest wall downward and the upper arm extended. The region of interest defined was centered on the scanner. To confirm reproducibility, two scans were acquired per site with slight changes to body position.

Three-dimensional images were created at a resolution of 1440 × 1440 pixels in a square area of 18 cm × 18 cm using imaging software[18] (Kurumi; Kyoto University, Kyoto, Japan). This software program can identify the surface of the skin using a virtual cloth. Using this program, the vessels were color-coded by depth (Supplementary Figure 1). The landmarks marked on the body surface were identified on the most superficial layer. These locational references were memorized digitally and shown in images of deeper layers. By removing the signals from the superficial layers, the subdermal venous network could be removed, thereby allowing the visualization of the subcutaneous vessels alone. Perforator branches that run toward the skin, become thin in the periphery, and have no connection with the venous network of polygonal tessellation morphology were defined as cutaneous (arterial) branches (Supplementary video).

When multiple perforators were observed in the region of interest, the largest perforator located closest to the lateral edge of the LD was characterized. To analyze the location of the stem portion of the perforator, an x-y orthogonal coordinate system was defined. The y-axis was defined as the caudally directed line on the lateral edge of the LD. The x-axis was defined as the dorsally directed line crossing the y-axis at a right angle at the level of the posterior axillary fold. The proximal base of the visualized perforator at the level corresponding to the depth of the deep fascia identified using ultrasound was defined as the stem portion. In addition to the x-y orthogonal coordinate system, a polar coordinate system was defined. The distribution of the longest cutaneous branch was analyzed using the polar coordinate system. The length and orientation of the direct length between the stem portion and the most distal portion of the branch were analyzed using the polar coordinate system. The relationship between the maximal depth of perforators delineated on photoacoustic images and the depth of the deep fascia from the skin surface was assessed.

Normally distributed data are presented as means ± standard deviation. The relationship between two continuous variables was evaluated using linear regression. The Wilcoxon rank sum test was used to compare nonparametric data from two independent samples. A p-value of < 0.05 was considered statistically significant.

Results

During the study period from 2018 to 2019, 11 healthy volunteers and 7 patients with benign breast disease were eligible. The study population included one man and 17 women, with a mean age of 44 ± 11 years (range, 21-62 years) and a mean body mass index of 21 ± 2 kg/m2 (range, 17-25 years). Images obtained with photoacoustic imaging at 34 sites in the lateral chest (17 sites on the right side and 17 sites on the left side) were analyzed.

The depths of the deep fascia and the deepest portion of the latissimus dorsi were 6 ± 3 mm (range, 3-14 mm) and 11 ± 4 mm (range, 6-20 mm), respectively, based on ultrasound measurements. In all study participants, perforators were identified in the region of interest. An average of 2.1 perforators (total, 71; range, 1-4 perforators) were observed in the region of interest. The course of perforators was tracked continuously from the submuscular layer to the layer just above the fascia. However, cutaneous branches were not identifiable clearly.

An average of 2.6 perforators (range, 1-5 perforators) were visualized in the region of interest using photoacoustic imaging. Of 71 perforators identified using ultrasound, 70 were delineated on photoacoustic images. By contrast, 5 of 34 large perforators were not identified using ultrasound. Representative images of TDAPs from photoacoustic imaging with various subcutaneous layer thicknesses are presented in Figure 1. The morphology of the perforators spreading in a dendritic form was delineated in three dimensions, especially when the subcutaneous layer was thick. The mean maximal depth of the perforators was 13 mm (range, 6-21 mm). In all study participants, the deepest part of the perforators was deeper than the level of the deep fascia identified using ultrasound (Figure 2a). The maximal depth of the perforator delineation was comparable to the depth of the deep portion of the latissimus dorsi (Figure 2b). This finding was inconsistent with the findings of a previous study[9], where visualization of anterolateral thigh perforators was limited to the depth of the deep fascia (Figure 3a). On average, the stem portion of the perforator was located 15 mm medial (range, −7 mm to 36 mm) to the lateral edge of the LD and 98 mm (range, 55-138 mm) caudal to the posterior axillary fold (Figure 3a). There was only one participant with the perforator located ventral to the lateral edge of the LD. Cutaneous branches of the perforator were distributed in a medial-caudal direction (range, 77-194°) (Figure 3b). The mean length of the longest cutaneous branch was 29 mm (range, 7-78 mm). Our measurements showed that the thicker the subcutaneous layer, the longer the cutaneous branch (Pearson's correlation coefficient, 0.72) (Supplementary Figure 2). In three subjects, long linking vessels were distributed transversely to connect to the dorsal perforator system (Figure 4). Intermuscular vessels were observed at 21 sites. These vessels were significantly delineated in subjects with a thin subcutaneous layer (Figure 5).

Discussion

In this study, we delineated TDAPs using photoacoustic imaging. The maximum depth of visualized perforators was 21 mm in the study participant with the thickest subcutaneous layer. Cutaneous branches distributed in a dendritic pattern were observed in three dimensions, but the visualized length of the perforators depended on the thickness

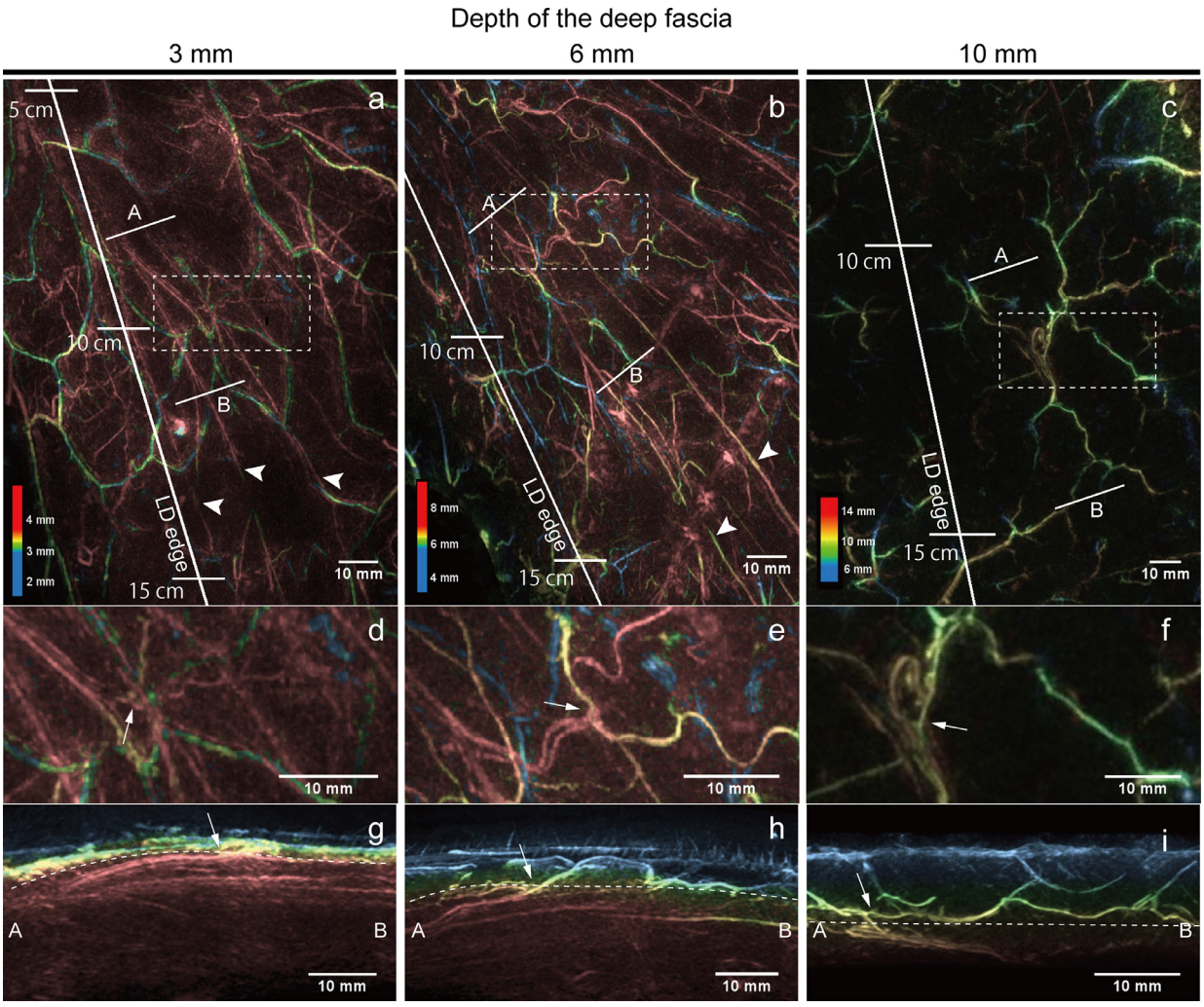

Figure 1 Three-dimensional photoacoustic imaging of thoracodorsal perforators in study participants with deep fascia of varying depth: 3, 6, and 10 mm. **a**–**c**) Photoacoustic images in the frontal view. All images are shown in the color degradation mode, with yellow indicating the depth of the deep fascia. The long lines represent the lateral edge of the LD. The short lines that intersect the LD line indicate the distance from the posterior axillary fold. The first perforators are shown in the rectangles. Note that intermuscular vessels were observed in study participants with a thin subcutaneous layer (arrowheads). **d**–**f**) Magnified images of the rectangles. The stem portions of the perforators are shown (arrows). **g**–**i**) Images in the lateral view for regions between **A** and **B** in the frontal view images. The broken lines represent the level of the deep fascia. Cutaneous branches above the fascia are visualized in blue-green. Note that long cutaneous branches were identified in a participant with a deep fascia depth of 10 mm, whereas cutaneous branches were not observed in a study participant with a deep fascia depth of 3 mm.

of the subcutaneous layer. The branches were mainly delineated in a medial-caudal direction.

Perforators from the descending branch of the thoracodorsal artery, transverse branch, and intercostal arteries spread throughout the lateral chest wall to form complex vascular networks in the subcutaneous layer.[1,19] Of note, the first perforator, which originates from the descending branch of the thoracodorsal artery, is reportedly the most dominant and reliable.[1,16,20] To describe where the first perforator emerges, several anatomical landmarks have been advocated. Angrigiani et al.[1] reported that it emerges 8 cm below the posterior axillary fold and 2 cm posterior to the lateral edge of the LD based on their anatomical dissection of 40 fresh cadavers. Heitmann et al.[16] identified the bifurcating point (vascular hilus) of the thoracodorsal artery 4 cm distal to the inferior scapular tip and 2.5 cm medial to the lateral edge of the LD based on a study of 20 fresh cadavers. In their specimens, all perforators originated within 8 cm from the hilus. Lin et al.[21] studied the reliability of these anatomical landmarks using ten clinical cases. Perforators were found within 1.5 cm from the site described by Angrigiani et al. in only five cases. Moreover, the thoracodorsal hilum was found around the site described by Heitmann et al. in only two cases. They attributed the uncertainty of anatomical landmarks for TDAPs to their mobility, possible differences between cadavers and living subjects, and anatomical variations associated with race, body size, and congenital or acquired skeletal deformities.

The uncertainty of TDAP-related landmarks has led to the need for a diagnostic modality to detect TDAP perforators

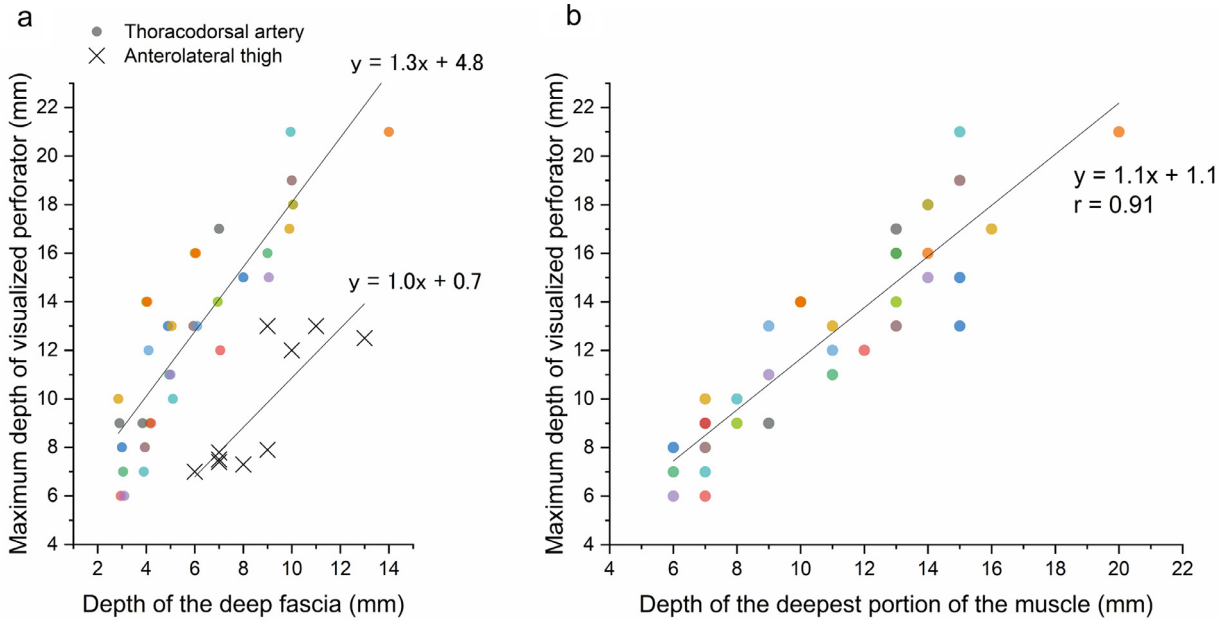

Figure 2 Scatter plots showing the relationship between the depth of the deep fascia from the skin surface and the maximum depth of perforators visualized using photoacoustic imaging (**a**) and the relationship between the depth of the deepest portion of the LD and the maximum depth of the perforators (**b**). Colored dots represent data from study participants in this study. Crosses represent data on anterolateral thigh perforators from participants of our previous study.[9] Overall, there is a relationship between deep fascia depth and maximum depth of the perforators in the anterolateral thigh. However, the maximal depth of the perforators exceeded the depth of the deep fascia but was very similar to the depth of the deepest portion of the muscle.

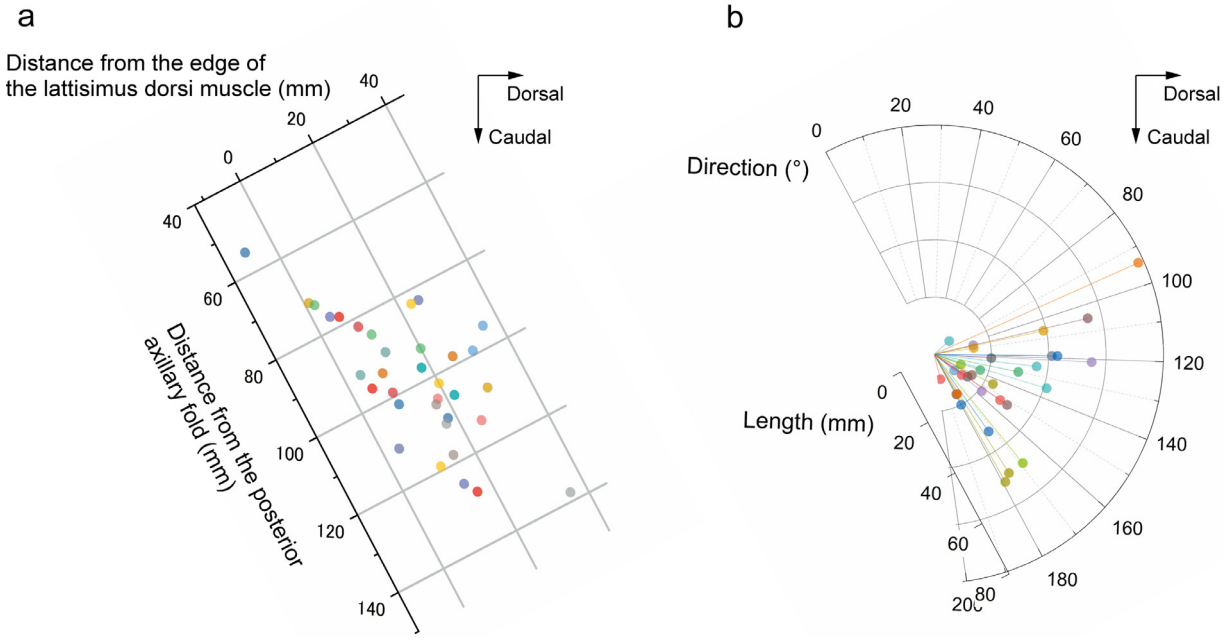

Figure 3 **a**) Scatter plots on the orthogonal coordinate system showing the location of the stem portion of the perforators delineated on photoacoustic images. **b**) The polar coordinate graph showing the direction and length of the main cutaneous branch of the perforators. The direction of the 0-180° axis corresponds to the direction of the lateral edge of the LD.

in vivo. Tashiro et al.[22] examined 7 TDAP flaps in 7 patients before surgery. Capillary perforators < 0.5 mm were visualized along the lateral edge of the LD, which were also identified intraoperatively. Although color Doppler ultrasound has advantages in that it is mobile and has high resolution, perforator visualization remains technically demanding. Onoda et al.[23] delineated the perforators of various flaps using multidetector computed tomography (MDCT). They found that visualization was especially difficult in patients with a subcutaneous layer thickness of ≤8 mm. Kim

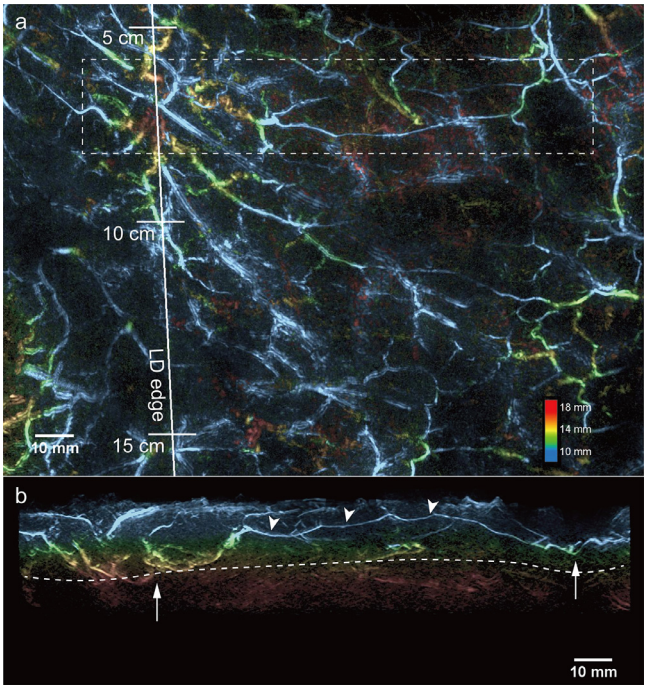

Figure 4 Linking vessels delineated on photoacoustic imaging. **a**) Photoacoustic image in the frontal view. The long white line indicates the lateral edge of the LD. The short lines indicate the distance from the posterior axillary fold. A cutaneous branch originates from the first perforator and courses transversely to connect to a perforator network on the dorsal side (rectangle). **b**) Lateral view of the linking vessel within the rectangle. The stem portions of ventral and dorsal perforator networks (arrows) communicate with each other via a cutaneous branch (arrowheads).

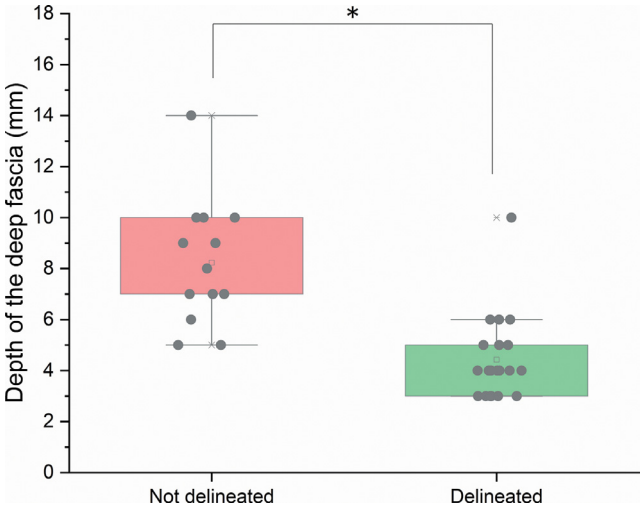

Figure 5 Box-and-whisker plots showing the relationship between intramuscular blood vessel delineation and depth of the deep fascia of the LD.

et al.[24] demonstrated improved perforator identification using MDCT with 0.8 mm slices based on multidirectional observation. Photoacoustic imaging is less invasive than MDCT. Moreover, three-dimensional visualization, high spatial resolution (0.5 mm), and short examination time (5 min per region of interest in this study) are strong advantages. Interestingly, 5 of 34 perforators with long cutaneous branches based on photoacoustic imaging were not identified using ultrasound. This might be due to the difficulty in searching for perforators comprehensively using ultrasound.

Knowledge of the distribution of cutaneous TDAP branches is important in designing flaps with large and complex morphology. Schaverien et al.[19] dissected cadavers and infused contrast medium directly into TDAPs to visualize them in three dimensions using MDCT. They delineated arterial and venous networks in the subcutaneous layer. TDAPs were distributed in a medial-caudal direction. The maximal length of the horizontal branch was 41 mm. The present study found a similar distribution of perforators. In study participants with a thick subcutaneous layer, long perforators were observed, with the longest being 78 mm. In study participants with a thin subcutaneous layer, visualization of cutaneous branches was very limited; intramuscular vessels were delineated instead. This finding was not consistent with a finding from a previous study[9] on anterolateral thigh perforators, where perforator delineation was limited to the level of the deep fascia despite the fact that the laser was theoretically expected to penetrate deeper than that level. This limited laser penetration was attributed to the thickness of the lateral fascia lata.[25] The thin deep fascia of the LD [26] might have been a cause of visualized intramuscular or submuscular vessels in this study.

Linking vessels between thoracodorsal and intercostal angiosomes are important anatomical structures that contribute to a large vascular territory of the lateral chest wall. Watanabe et al.[27] investigated the perfusion system in the entire LD and overlying subcutaneous layers using fresh cadavers. Three vascular territories were identified. They suggested the importance of chock (linking) vessels connecting the first (most proximal) and second (middle) vascular territories. Schaverien et al.[15] delineated the linking vessels between thoracodorsal and dorsal intercostal angiosomes in three dimensions using cadavers with a barium sulfate and gelatin mixture injection method. Vascular networking occurred through the subdermal plexus, not the suprafascial plexus. In this study, the linking vessel between the lateral (thoracodorsal) and medial (dorsal intercostal) perforator systems was observed in three dimensions. This is the first report to delineate linking vessels *in vivo* in three dimensions. Information on the three-dimensional morphology of cutaneous TDAP branches and their networks with neighboring vascular territories provided by photoacoustic imaging might be useful in flap design and thinning. Recently, vascular mapping based on photoacoustic imaging technology was used in anterolateral thigh thin flap surgery, which was found to be accurate and useful.[28] A detailed map of the thoracodorsal perforator perfusion system might contribute to more advanced TDAP surgery with larger skin paddles of more complicated morphology.

This study had some technical limitations. Perforators from thoracodorsal arteries have varying courses (*i.e.*, mus-

culocutaneous or septocutaneous). In cadaveric dissections performed by Thomas et al.,[7] a mean of 5.5 TDAPs were found in the region caudal to the inferior angle of the scapula, and the ratio of the musculocutaneous to septocutaneous perforators was 3.2. In the present study, we did not discriminate between these two types of perforators because soft tissue is not visualized on photoacoustic images. Moreover, there was a possibility that perforating branches from the ninth intercostal artery[25] might have been considered perforators in the region of interest defined in this study, especially perforators located more inferior and close to the lateral edge of the LD. Concomitant conventional ultrasound might enhance the diagnostic accuracy of perforator identification based on photoacoustic imaging.

Declaration of Competing Interest

The authors declare no conflicts of interest in association with the present study.

The author(s) used a photoacoustic imaging system made by Canon Inc., Tokyo, Japan.

Acknowledgements

The authors thank Tomoko Kosaka, Tomoko Ishii, Kazuko Kobayashi, Minako Chaya, Goshiro Yamamoto, Takeshi Namita, Tsuyoshi Shiina, Yoshiaki Matsumoto, Masahiro Takada, Norihiko Utsunomiya, Kenichi Nagae, Satoru Fukushima, Shuich Kobayashi, Yasufumi Asao, and Takayuki Yagi for their assistance.

Funding

This work was funded by the ImPACT Program of the Council for Science, Technology and Innovation (Cabinet Office, Government of Japan). This study was also supported by AMED under Grant Number JP22he2302002.

Ethical approval

This study was conducted with the approval of the ethics review board of Kyoto University Graduate School of Medicine, Kyoto, Japan (approval number: C1366).

Author Contributions

Hanako Shimizu: performed examinations, analyzed the data and wrote the manuscript. Susumu Saito: designed the study, analyzed the data and wrote the manuscript. All the authors interpreted the data and reviewed the manuscript.

Supplementary materials

Supplementary material associated with this article can be found, in the online version, at doi:10.1016/j.bjps.2022.06.016.

References

1. Angrigiani C, Grilli D, Siebert J. Latissimus dorsi musculocutaneous flap without muscle. *Plast Reconstr Surg* 1995;**96**:1608–14.
2. Hamdi M, Van Landuyt K, Monstrey S, Blondeel P. Pedicled perforator flaps in breast reconstruction: a new concept. *Br J Plast Surg* 2004;**57**:531–9.
3. Koshima I, Narushima M, Mihara M, et al. New thoracodorsal artery perforator (TAPcp) flap with capillary perforators for reconstruction of upper limb. *J Plast Reconstr Aesthet Surg* 2010;**63**:140–5.
4. O'Connell JE, Bajwa MS, Schache AG, Shaw RJ. Head and neck reconstruction with free flaps based on the thoracodorsal system. *Oral Oncol* 2017;**75**:46–53.
5. Kim EJ, Lee KT, Lim SY, et al. Reconstructing facial contour deformities using stereoscopic thoracodorsal artery perforator adipofascial flaps. *Microsurgery* 2017;**37**:300–6.
6. Arikawa M, Miyamoto S, Fujiki M, Higashino T, Oshima A, Sakuraba M. Comparison of donor site drainage duration and seroma rate between latissimus dorsi musculocutaneous flaps and thoracodorsal artery perforator flaps. *Ann Plast Surg* 2017;**79**:183–5.
7. Thomas BP, Geddes CR, Tang M, Williams J, Morris SF. The vascular basis of the thoracodorsal artery perforator flap. *Plast Reconstr Surg* 2005;**116**:818–22.
8. Wang LV, Hu S. Photoacoustic tomography: *in vivo* imaging from organelles to organs. *Science* 2012;**23**:1458–62 335.
9. Tsuge I, Saito S, Sekiguchi H, et al. Photoacoustic tomography shows the branching pattern of anterolateral thigh perforators In Vivo. *Plast Reconstr Surg* 2018;**141**:1288–92.
10. Saito S, Bise R, Yoshikawa A, Sekiguchi H, Tsuge I, Toi M. Digital artery deformation on movement of the proximal interphalangeal joint. *J Hand Surg Eur* 2019;**44**:187–95 *Vol.*.
11. Toi M, Asao Y, Matsumoto Y, et al. Visualization of tumor-related blood vessels in human breast by photoacoustic imaging system with a hemispherical detector array. *Sci Rep* 2017;**7**:41970.
12. Yamaga I, Kawaguchi-Sakita N, Asao Y, et al. Vascular branching point counts using photoacoustic imaging in the superficial layer of the breast: a potential biomarker for breast cancer. *Photoacoustics* 2018;**11**:6–13.
13. Nagae K, Asao Y, Sudo Y, et al. Real-time 3D photoacoustic visualization system with a wide field of view for imaging Human Limbs. *F1000Res* 2018;**7**:1813.
14. Mun GH, Lee SJ, Jeon BJ. Perforator topography of the thoracodorsal artery perforator flap. *Plast Reconstr Surg* 2008;**121**:497–504.
15. Schaverien M, Saint-Cyr M, Arbique G, Brown SA, Rohrich RJ. Three- and four-dimensional arterial and venous anatomies of the thoracodorsal artery perforator flap. *Plast Reconstr Surg* 2008;**121**:1578–87.
16. Heitmann C, Guerra A, Metzinger SW, Levin LS, Allen RJ. The thoracodorsal artery perforator flap: anatomic basis and clinical application. *Ann Plast Surg* 2003;**51**:23–9.
17. American national standard for safe use of lasers: American National Standards Institute, 2014. https://www.ansi.org/ (10 June 2015).
18. Sekiguchi H, Yoshikawa A, Matsumoto Y, et al. Body surface detection method for photoacoustic image data using cloth-simulation technique. In: Proceedings of the SPIE BiOS, *San Franciso, California*; February 19, 2018.
19. Schaverien M, Wong C, Bailey S, Saint-Cyr M. Thoracodorsal artery perforator flap and Latissimus dorsi myocutaneous flap-anatomical study of the constant skin paddle perforator locations. *J Plast Reconstr Aesthet Surg* 2010;**63**:2123–7.
20. Guerra AB, Metzinger SE, Lund KM, Cooper MM, Allen RJ, Dupin CL. The thoracodorsal artery perforator flap: clinical ex-

perience and anatomic study with emphasis on harvest techniques. *Plast Reconstr Surg* 2004;**114**:32–41.
21. Lin CT, Huang JS, Yang KC, et al. Reliability of anatomical landmarks for skin perforators of the thoracodorsal artery perforator flap. *Plast Reconstr Surg* 2006;**118**:1376–86.
22. Tashiro K, Yamashita S, Araki J, Narushima M, Iida T, Koshima I. Preoperative color Doppler ultrasonographic examination in the planning of thoracodorsal artery perforator flap with capillary perforators. *J Plast Reconstr Aesthet Surg* 2016;**69**:346–50.
23. Onoda S, Azumi S, Hasegawa K, Kimata Y. Preoperative identification of perforator vessels by combining MDCT, doppler flowmetry, and ICG fluorescent angiography. *Microsurgery* 2013;**33**:265–9.
24. Kim JG, Lee SH. Comparison of the Multidetector-row Computed tomographic angiography axial and coronal planes' usefulness for detecting thoracodorsal artery perforators. *Arch Plast Surg* 2012;**39**:354–9.
25. Pirri C, Fede C, Petrelli L. An anatomical comparison of the fasciae of the thigh: a macroscopic, microscopic and ultrasound imaging study. *J Anat* 2021;**238**:999–1009.
26. Bogduk N, Johnson G, Spalding D. The morphology and biomechanics of latissimus dorsi. *Clin Biomech (Bristol, Avon)* 1998;**13**:377–85.
27. Watanabe K, Kiyokawa K, Rikimaru H, et al. Anatomical study of latissimus dorsi musculocutaneous flap vascular distribution. *J Plast Reconstr Aesthet Surg* 2010;**63**:1091–8.
28. Tsuge I, Saito S, Yamamoto G, et al. Preoperative vascular mapping for anterolateral thigh flap surgeries: a clinical trial of photoacoustic tomography imaging. *Microsurgery* 2020;**40**:324–30.